Rational Design of Peptide Inhibitors of the Sarcoplasmic Reticulum Calcium Pump†

Michael R. Afara, Catharine A. Trieber, John Paul Glaves, and Howard S. Young*

Department of Biochemistry, University of Alberta, Edmonton, Alberta, Canada T6G 2H7

Received November 21, 2005; Revised Manuscript Received May 16, 2006

ABSTRACT: The sequence of phospholamban (PLB) is practically invariant among mammalian species. The hydrophobic transmembrane domain has 10 leucine and 8 isoleucine residues. Two roles have been proposed for the leucines; one subset stabilizes PLB oligomers, while a second subset physically interacts with SERCA. On the basis of the sequence of the PLB transmembrane domain, we chemically synthesized a series of peptides and tested their ability to regulate SERCA in reconstituted membranes. In all, eight peptides were studied: a peptide corresponding to the null-cysteine transmembrane domain of PLB (TM-Ala-PLB), two polyleucine peptides (Leu_{18} and Leu_{24}), polyalanine peptides containing 4, 7, and 12 leucine residues (Leu_4, Leu_7, and Leu_{12}, respectively), and a polyalanine peptide containing the 9 leucine residues present in the transmembrane domain of PLB with and without the essential Asn^{34} residue (Asn_1Leu_9 and Leu_9, respectively). With the exception of Leu_{18}, co-reconstitution of the peptides revealed effects on the apparent calcium affinity of SERCA. The TM-Ala-PLB peptide possessed approximately 70% of the inhibitory function of wild-type PLB. The remaining peptides exhibited significant inhibitory activity decreasing in the following order: Leu_{12}, Leu_9, Leu_{24}, Leu_7, and Leu_4. Replacing Asn^{34} of PLB in the Leu_9 peptide resulted in superinhibition of SERCA. On the basis of these observations, we conclude that a partial requirement for SERCA inhibition is met by a simple hydrophobic surface on a transmembrane α-helix. In addition, the superinhibition observed for the Asn^{34}-containing peptide suggests that the model peptides mimic the inhibitory properties of PLB. A model is presented in which surface complementarity around key amino acid positions is enhanced in the interaction with SERCA.

The dynamic control of intracellular calcium stores differentiates cardiac contractility from that in the neuromusculature. In both heart and skeletal muscle, the sarcoplasmic reticulum (SR)[1] supplies calcium for muscle contraction and sequesters calcium for muscle relaxation. Uptake of calcium into the lumen of the SR determines the rate of muscle relaxation and the size of the calcium store that is available for the subsequent contraction. In both muscle types, this is accomplished by an ATP-dependent calcium pump, SERCA. The calcium pump plays a central role in calcium handling and in the cyclic release and reuptake of SR calcium. In heart muscle, major modifications of contractility involve phospholamban (PLB) and sarcolipin (SLN). PLB and SLN are small integral membrane proteins that interact with SERCA and dynamically regulate the contraction−relaxation cycle (*1*−*3*). SLN is a skeletal muscle homologue of PLB, which is also expressed in the atrial myocardium (*4*). The atrium-specific regulation of SERCA may involve a ternary super-inhibitory complex with PLB and SLN (*5*), thereby differentiating the contractile properties of the atria from those of the ventricles. Both proteins physically interact with the SERCA, altering its calcium affinity and modulating cardiac contractility in response to stress, exercise, and disease.

The molecular mechanism by which PLB slows the recovery of calcium by the cardiac SERCA has been studied in great detail. Physical interactions between PLB and SERCA decrease the apparent calcium affinity of the pump by a mechanism that increases the activation energy for a calcium-dependent transition (*6*). Every amino acid in the primary sequence of PLB has been mutated to alanine, providing valuable insight into the importance of individual amino acids in the functional interaction with SERCA (*7*, *8*). Recent efforts have successfully expanded these studies to reconstitution systems (*9*, *10*), where the molecular mechanism of calcium pump regulation by PLB can be characterized in a chemically pure membrane environment. For the inhibitory function of the transmembrane domain of PLB, eight amino acids can be considered essential. When

† This work was supported by grants from the Heart and Stroke Foundation of Alberta, the Canada Foundation for Innovation, and the Alberta Science and Research Investments Program. H.S.Y. is a Scholar of the Alberta Heritage Foundation for Medical Research and a New Investigator of the Canadian Institutes of Health Research.

* To whom correspondence should be addressed. Phone: (780) 492-3931. Fax: (780) 492-0095. E-mail: hyoung@ualberta.ca.

[1] Abbreviations: $C_{12}E_8$, octaethylene glycol monododecyl ether; EYPA, egg yolk phosphatidic acid; EYPC, egg yolk phosphatidylcholine; SOPC, stearoyl-2-oleoylphosphatidylcholine; K_{Ca}, calcium concentration at half-maximal activity; n_H, Hill coefficient; PLB, phospholamban; SLN, sarcolipin; SR, sarcoplasmic reticulum; SERCA, sarco(endo)plasmic reticulum calcium ATPase; V_{max}, maximal activity; TFA, trifluoroacetic acid; CH_3CN, acetonitrile; CD, circular dichroism; TM-Ala-PLB, transmembrane domain of phospholamban with cysteine residues substituted with alanine residues; Leu_{18}, acetyl-K_2-L_{18}-K_2-amide; Leu_{24}, acetyl-K_2-L_{24}-K_2-amide; Leu_4, acetyl-K_2-$(LAAAAAA)_3$-LAA-K_2-amide; Leu_7, acetyl-K_2-$(LAAALAA)_3$LAA-K_2-amide; Leu_{12}, acetyl-K_2-$(LA)_{12}$-K_2-amide; Leu_9, acetyl-K_2-LAALAAAAALALAALL-LAAAAAALL-K_2-amide; Asn_1Leu_9, acetyl-K_2-LAALAANAALA-LAALLLAAAAAALL-K_2-amide; ANOVA, analysis of variance.

10.1021/bi0523761 CCC: $33.50
Published on Web 06/21/2006

individually mutated to alanine, amino acids Leu[31], Asn[34], Phe[35], Ile[38], Leu[42], Ile[48], Val[49], and Leu[52] yield loss-of-function mutants (*7*). More complex mutagenesis studies of PLB are rare, but a few double mutants have been characterized (*7*, *11*, *12*). When the N34A loss-of-function mutation was combined with the N27A gain-of-function mutation, the double mutant regained ~50% inhibitory activity; however, a double mutant combining the N34A mutation with the I40A gain-of-function mutation was completely noninhibitory (*11*, *12*). As another example, combining the F35A loss-of-function mutation and the L44A gain-of-function mutation resulted in a net improvement in inhibitory activity (*7*). Last, combination of the L31A loss-of-function mutation with either the N27A or the N30A gain-of-function mutation did not restore inhibitory function. We conclude that the inhibitory properties of individual amino acids are context-dependent and that it is the complex interaction of key residues with SERCA that modulates calcium reuptake and cardiac contractility.

Monotopic integral membrane proteins such as PLB are characterized by a single membrane-spanning α-helix with a conformation and orientation influenced by the membrane bilayer. For PLB, the transmembrane segment undergoes a transition from predominantly lipid interactions to a SERCA-bound state, presumably through the association of the hydrophobic α-helices of both proteins. In their lipid bilayer interactions, such helical transmembrane segments may be tilted with respect to the plane of the membrane and typically consist of a stretch of at least 20 hydrophobic amino acids. This is certainly the case for the pentameric form of PLB (*13*). To understand the membrane association of a typical transmembrane sequence, polyleucine-containing peptides have been studied as canonical transmembrane α-helices. This work has resulted in the molecular description of the partitioning and association of a canonical transmembrane α-helix with model membrane bilayers (*14*−*22*). Two such peptides have been well-characterized: a polyleucine peptide and an alternating leucine-alanine peptide, the hydrophobic cores of which are both 24 amino acids in length. With the realization that the sequence of a polyleucine helix bears a remarkable similarity to those of the transmembrane domains of PLB and SLN, we tested the ability of such peptides to interact with SERCA.

Of the eight essential amino acids in the transmembrane domain of PLB, three are leucines and the majority are hydrophobic. Moreover, the transmembrane domain of PLB is extremely hydrophobic with the exception of the essential residue Asn[34] (*7*, *9*) and the three nonessential cysteine residues (*23*). Therefore, one component of the intramembrane interaction that results in SERCA inhibition may be van der Waals interactions that mediate specific associations between transmembrane helices. In the case of PLB, a simple hydrophobic surface may then facilitate the more specific interaction of the essential residues (Leu[31], Asn[34], Phe[35], Ile[38], Leu[42], Ile[48], Val[49], and Leu[52]), mutation of which abolishes PLB function. To test this hypothesis, we have focused on the role of leucine residues in forming a canonical hydrophobic surface for functional interaction with SERCA. Peptides containing 4−12 leucine residues on a transmembrane helix are shown to decrease the apparent calcium affinity of SERCA. Replacement of Asn[34] in one of these peptides shifted the inhibitory capacity from a relatively weak inhibition to superinhibition. We conclude that a simple hydrophobic surface satisfies a partial requirement for SERCA inhibition and that the peptides mimic the reversible inhibition by the transmembrane domain of PLB.

EXPERIMENTAL PROCEDURES

Materials. Octaethylene glycol monododecyl ether ($C_{12}E_8$) was obtained from Barnet Products (Englewood Cliffs, NJ). SM-2 Biobeads were obtained from Bio-Rad (Hercules, CA). Egg yolk phosphatidylcholine (EYPC), egg yolk phosphatidic acid (EYPA), and 1-stearoyl-2-oleoylphosphatidylcholine (SOPC) were obtained from Avanti Polar Lipids (Alabaster, AL). All the reagents used in the coupled enzyme assay (*24*) for measuring ATPase activity were of the highest available purity (Sigma-Aldrich, Oakville, ON).

Peptide Synthesis and Purification. Peptide synthesis was carried out by the Alberta Peptide Institute (API, University of Alberta). Briefly, peptides were synthesized on an ABI 433A peptide synthesizer (Applied Biosystems, Foster City, CA) following standard synthesis protocols (0.1 mm scale) (*16*). The crude product was dissolved in 20−30% CH_3CN and purified on a Zorbax 300SB-C8 reverse-phase column eluting with buffer A and a 1% per minute linear gradient of buffer B (buffer A was 0.05% TFA and buffer B was 0.5% TFA/CH_3CN). Peptide fractions were identified by matrix-assisted laser desorption ionization time-of-flight (Voyager DE Pro, Applied Biosystems, Foster City, CA) mass spectrometry. Pure fractions were pooled and lyophilized, and the purified product was quantitated by amino acid analysis.

CD Spectroscopy. CD spectra were measured at 20 °C on a Jasco J-500C spectropolarimeter (Jasco, Easton, MD). The instrument was routinely calibrated with an aqueous solution of recrystallized d_{10}-(+)-camphosulfonic acid (*16*). The data were collected at 0.1 nm resolution with a scan speed of 50 nm/min from 250 to 190 nm in quartz cells with a path length of 0.02 cm. A simple spline curve of the data was generated with Sigma Plot (SPSS Inc., Chicago, IL). Peptide concentrations were 1.5 mg/mL, and spectra were measured in lipid vesicles. In the preparation of lipid vesicles, the peptide and SOPC were solubilized in distilled methanol in a 1:30 ratio, dried to a thin film under nitrogen gas, and lyophilized. Buffer [100 mM phosphate (pH 7.0)] was added followed by vigorous vortexing to rehydrate the mixture. The mixture was then extruded through a 100 nm filter to form large multilamellar vesicles approximately 100 nm in diameter.

Reconstitution of SERCA and Peptides. Skeletal muscle SR vesicles were prepared from rabbit hind leg (*25*), and the skeletal SR SERCA was purified by Reactive-Red affinity chromatography as described previously (*26*). Functional reconstitution of SERCA with PLB has been described previously (*27*−*29*). For these studies, 40−54 μg of peptide, 315 μg of EYPC, and 35 μg of EYPA were solubilized in organic solvent (1 part TFE and 2 parts chloroform), dried to a thin film under nitrogen gas, and lyophilized. Buffer [20 mM imidazole (pH 7.0), 100 mM KCl, 0.02% NaN_3] and a total of 700 μg of detergent ($C_{12}E_8$) were added followed by vigorous vortexing to solubilize the mixture. To the suspension of peptide and lipids was added 300 μg of pure SERCA. The final volume was adjusted to 300 μL, and the concentrations were adjusted such that the final

amounts were 350 μg of protein, 350 μg of lipid, and 700 μg of detergent (final SERCA:peptide:lipid molar ratio of 1:5:150). The detergent was removed by incremental addition of SM-2 Biobeads over a 4 h time course. The co-reconstituted proteoliposomes containing SERCA and peptide were purified on a sucrose step gradient (*9*, *28*). The molar ratios of peptide to SERCA were determined by quantitative SDS−PAGE as described (*9*, *30*, *31*). Briefly, incremental amounts of purified peptide (quantitated by amino acid analysis) and SERCA were run next to the proteoliposomes on a polyacrylamide gel. After Coomassie staining, gels were digitized with an Epson (Toronto, ON) Perfection 3200 densitometer, and bands were quantitated, after background subtraction, with ImageQuant. Standard curves were constructed from the known quantities of peptide and SERCA, and the unknown proteoliposome samples were quantitated by comparison to the standards. For peptide quantitation, staining was improved with the use of Coomassie Blue G-250 (GelCode, Pierce, Rockford, IL), after fixing was carried out in 40% methanol and 7.5% acetic acid. Finally, the lipid:protein ratios were determined as described previously (*28*, *32*, *33*).

ATPase Activity Measurements. ATPase activity of the co-reconstituted vesicles was measured by a coupled enzyme assay (*24*). All co-reconstituted membranes were matched to controls, and each assay was performed multiple times ($n = 3-5$ for peptide-containing samples; $n = 17$ for matched SERCA controls) over a range of free calcium concentrations from 0.1 to 10 μM. Recently, our method has been described in detail (*9*, *34*). Data were plotted as the ATPase specific activity (micromoles of ATP hydrolyzed per milligram of SERCA per minute) versus pCa (negative log of the Ca^{2+} concentration). The K_{Ca} (calcium concentration at half-maximal activity), V_{max} (maximal activity), and Hill coefficient (n_H) were calculated on the basis of nonlinear least-squares fitting of the activity data (V vs Ca^{2+} concentration in micromolar) to the Hill equation, $V = V_{max}[Ca]^{n_H}/(K_{Ca}{}^{n_H} + [Ca]^{n_H})$, using Sigma Plot (SPSS Inc.). Errors are the standard error of the mean for a minimum of three independent measurements. Comparison of K_{Ca}, n_H, and V_{max} parameters was carried out using ANOVA (between subjects, one-way analysis of variance) followed by Tukey's HSD post hoc test for pairwise comparisons. In all cases, control samples were as follows: (i) negative control, SERCA reconstituted in the absence of peptide; (ii) negative control, SERCA co-reconstituted in the presence of a noninhibitory polyleucine peptide (Leu_{18}, Figure 1); (iii) positive control, SERCA co-reconstituted in the presence of the transmembrane domain of PLB (TM-Ala-PLB, Figure 1); and (iv) positive control, SERCA co-reconstituted in the presence of full-length, wild-type PLB.

Kinetic Analysis. A detailed reaction scheme and rate constants have been described for the transport cycle of SERCA in the absence and presence of PLB inhibition (*6*). We performed a global nonlinear regression fit of this proposed model to the SERCA activity curves in the absence and presence of peptides, obtained over a range of calcium concentrations (Dynafit from Biokin, Inc., Pullman, WA) (*35*). The SERCA activity curve in the absence of peptide was fit remarkably well with the exception of the rate constants for the two calcium binding steps, which were somewhat lower than the initially reported values. For our reconstituted SERCA proteoliposomes, $A_{forward}$ was determined to be 3×10^5 s^{-1} and $C_{forward}$ to be 2×10^6 s^{-1}. SERCA activity curves in the presence of either PLB or peptides could be easily fit with modifications to the rate constants for the slow isomeric transition following binding of the first calcium ion ($B_{forward}$ and $B_{reverse}$).

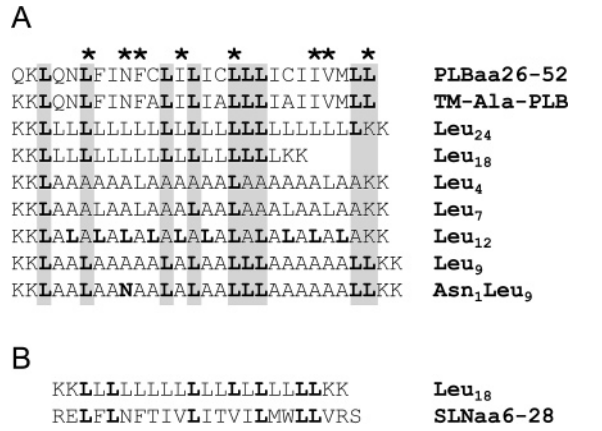

FIGURE 1: (A) Sequence alignment of the peptides used in this study, compared to the transmembrane domain of PLB (amino acid residues 26−52). Conserved leucine residues are highlighted in gray. The essential amino acids of PLB are denoted with asterisks. (B) Sequence alignment of the Leu_{18} peptide with the transmembrane domain of SLN (amino acid residues 6−28).

RESULTS

Synthetic Peptides. Synthetic leucine-based peptides, such as Leu_{24} and Leu_{12}, have been successfully utilized as models of the hydrophobic transmembrane segments of integral membrane proteins (*14*−*22*, *36*, *37*). These peptides are α-helical in a membrane bilayer and are anchored to the membrane surface by lysine residues that cap either end of the peptide. Interestingly, a sequence alignment of Leu_{24} with the transmembrane domain of PLB revealed a 35% identical and 73% similar sequence (for a 26-amino acid overlap; Figure 1). These facts prompted us to examine a variety of leucine-containing peptides for their ability to inhibit SERCA. The hypothesis to be tested was whether a canonical, uniform hydrophobic surface could satisfy part of the requirement for SERCA inhibition. If this hypothesis were correct, we would expect a specific peptide inhibitor of SERCA to mimic PLB and SLN function and to meet the following criteria: (i) Synthetic peptides substantially shorter than the transmembrane domains of PLB and SLN (~22 amino acids in length) should be noninhibitory; (ii) the synthetic peptides should inhibit SERCA at equimolar stoichiometries; and (iii) the synthetic peptides should mimic the amino acid sequence dependence of SERCA inhibition by PLB and SLN.

The eight peptides utilized in this study are shown in Figure 1. As a positive control for comparison to the synthetic peptides, we first synthesized the transmembrane domain of PLB lacking the three nonessential cysteine residues (*23*, *38*). Two polyleucine peptides were synthesized to test the length of the transmembrane segment required for SERCA inhibition (Leu_{18} and Leu_{24}). Three additional peptides containing between 4 and 12 leucine residues distributed over an alanine-based sequence that was either 24 or 25 amino acids in length (Leu_4, Leu_7, and Leu_{12}) were synthesized. Specif-

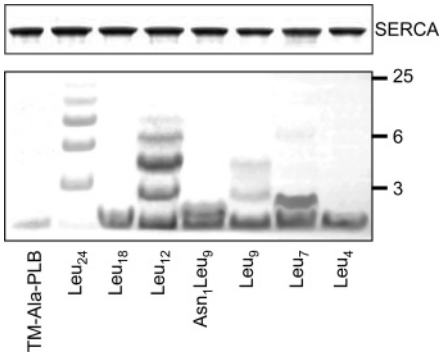

FIGURE 2: Coomassie-stained SDS−PAGE of co-reconstituted proteoliposomes containing SERCA and peptide. Co-reconstituted proteoliposomes were run on 10% (top) and 16% (bottom) polyacrylamide gels. Since the peptides stained weakly, a 5-fold larger amount of sample was loaded on a 16% gel for display purposes. Molecular mass markers (kilodaltons) are indicated. Leu_7 and Asn_1Leu_9 form monomers and dimers; Leu_9 forms monomers, dimers, and trimers, and Leu_{12} and Leu_{24} form a series of oligomeric species from pentamers to monomers.

ically, Leu_4 and Leu_7 possessed four or seven leucine residues lining one face of a transmembrane helix, and Leu_{12} possessed 12 leucine residues distributed around the circumference of the transmembrane helix. Finally, two additional polyalanine peptides that contained the nine leucine residues present in the transmembrane domain of wild-type PLB were synthesized, with and without essential polar residue Asn^{34} (Asn_1Leu_9 and Leu_9, respectively).

To support the hypothesis of a uniform hydrophobic surface on a canonical transmembrane helix, CD spectroscopy was utilized to examine the secondary structural characteristics of a subset of the peptides used in this study. The Leu_{24} and Leu_{12} peptides have already been shown to form hydrophobic α-helices in model lipid bilayers (*14*−*22*). Given the aqueous solubility of the Leu_4, Leu_7, and Leu_9 peptides, we examined the secondary structure adopted by these peptides in lipid bilayers. The peptides quantitatively partitioned into and remained associated with reconstituted proteoliposomes in the presence or absence of SERCA, as measured by quantitative SDS−PAGE (Figure 2 and Table 1). Furthermore, CD spectra were recorded for these peptides in model lipid vesicles (Figure 3), and they were identical to those previously recorded for PLB and SLN (*39*, *40*). In all cases, the spectra were similar to one another and were consistent with a high α-helical content (minima at 208 and 222 nm). Therefore, we conclude that the synthetic peptides studied herein traverse the membrane bilayer as an α-helix, much like the transmembrane domains of PLB and SLN.

Reconstituted Proteoliposomes. Reconstitution of SERCA at low lipid:protein ratios mimics the environment in native SR membranes and is a useful tool for structure−function studies in the absence and presence of PLB (*9*, *28*−*30*). Measurement of rates of ATP hydrolysis by reconstituted SERCA proteoliposomes yielded a K_{Ca} of 6.42 ± 0.01 pCa units (0.38 μM Ca^{2+}) and a V_{max} of 4.3 ± 0.3 μmol mg^{-1} min^{-1} ($n = 17$) at saturating calcium concentrations (2.5 μM Ca^{2+}). This activity was consistent with previous observations and served as one of the negative controls for all further studies in the presence of peptides (*9*). To verify that the co-reconstitution of SERCA and synthetic peptides was comparable to our previous studies with PLB, we examined the efficiency of reconstitution for all peptides in terms of the peptide:SERCA and lipid:protein molar ratios (Table 1) (*9*, *30*). After co-reconstitution and purification, the proteoliposomes contain a lipid:protein molar ratio of approximately of 120:1 and a peptide:SERCA molar ratio of approximately 4.5:1. The orientation of the peptide in the membrane is not known, but at this ratio of peptide to SERCA, assuming no bias exists in peptide incorporation, there should be two to three peptide molecules correctly oriented to interact with SERCA. Therefore, we conclude that the reconstituted proteoliposomes used herein were identical to those previously characterized (*9*, *29*, *30*, *34*) and were suitable for studying novel peptide inhibitors of SERCA.

Transmembrane Domain of PLB. As a positive control for our studies with the leucine-containing model peptides, we first synthesized the transmembrane domain of human PLB (residues 26−52). To improve the solubility of the peptide, alanine residues were substituted for the nonessential cysteine residues (Cys^{36}, Cys^{41}, and Cys^{46}) and a lysine residue was substituted for Gln^{26} (Figure 1). A comparable peptide has been shown to inhibit SERCA, albeit to a lesser extent than wild-type PLB (*38*, *41*). The functional effects of the TM-Ala-PLB peptide were tested in co-reconstituted membranes with SERCA (Figure 4 and Table 1), shifting the affinity of SERCA from approximately 0.38 to 0.59 μM calcium. This level of inhibition is approximately 70% of that of wild-type PLB (0.7 μM), consistent with previous observations (*38*, *41*). The maximal activity of SERCA was unaffected by the TM-Ala-PLB peptide, in contrast to previous observations with wild-type PLB (*9*, *10*). In terms of the observed effect on K_{Ca}, the TM-Ala-PLB peptide had a high statistical probability of being distinct from SERCA in the absence of peptide ($p < 10^{-2}$).

Polyleucine Peptides. Synthetic polyleucine peptides have served as models for the hydrophobic transmembrane α-helical segments of integral membrane proteins (*14*−*22*). In our studies, the peptides contained a long sequence of hydrophobic leucine residues (Leu_{18} and Leu_{24}) capped at both the N- and C-termini with two lysine residues (acetyl-K_2-L_{18}-K_2-amide and acetyl-K_2-L_{24}-K_2-amide). The polyleucine region of these peptides forms a stable α-helix with a uniform hydrophobic surface. In a membrane environment, the lysine residues anchor the ends of these peptides to the polar surfaces of the lipid bilayer. The charge repulsion of the lysine caps reportedly limits oligomerization of the peptides; however, oligmeric species were observed by SDS−PAGE (Figure 2). The polyleucine stretch of 18 residues (Leu_{18}) meets the minimum requirement for traversing the lipid bilayer as an α-helix, while a polyleucine stretch of 24 residues (Leu_{24}) more closely approximates the length of the PLB transmembrane domain. In comparison to PLB, the Leu_{24} peptide preserved the length, hydrophobicity, and N-terminal polarity of the transmembrane domain. In contrast, the Leu_{18} peptide preserved the hydrophobicity and N-terminal polarity but was significantly shorter than the transmembrane domain of PLB. The Leu_{18} peptide is one amino acid shorter than the transmembrane domain of SLN, and the lysine caps are similar to residues that flank the SLN transmembrane domain (Figure 1B). The capping lysine residues on both peptides make it unlikely that the C-terminus can reside in the interior of the membrane bilayer (*18*, *42*).

Table 1: Summary of the Data for Peptide Inhibitors of SERCA

peptide	peptide/SERCA[a]	lipid/protein[b]	K_{Ca} (μM)[c]	V_{max}[d]	kinetic analysis[e]		
					$B_{forward}$	$B_{reverse}$	sum of squares
control		0.76 ± 0.05	0.38 ± 0.01	4.3 ± 0.3 (10.1 ± 0.5)	30	40	0.002
wild-type PLB	4.7 ± 0.5	0.84 ± 0.02	0.68 ± 0.03	7.5 ± 0.1 (9.9 ± 0.1)	50	8×10^5	0.03
TM-Ala-PLB	3.7 ± 0.5	0.89 ± 0.03	0.59 ± 0.03	4.3 ± 0.4 (ND)	30	3×10^5	0.02
Leu_{18}	ND	0.73 ± 0.06	0.38 ± 0.01	2.8 ± 0.1 (ND)	19	40	0.004
Leu_{24}	4.9 ± 0.2	0.85 ± 0.09	0.54 ± 0.02	2.3 ± 0.3 (9.0 ± 0.1)	16	3×10^5	0.007
Leu_4	5.5 ± 0.6	0.83 ± 0.06	0.49 ± 0.01	6.2 ± 0.3 (9.7 ± 0.2)	46	2×10^5	0.03
Leu_7	5.1 ± 0.6	0.86 ± 0.06	0.50 ± 0.01	6.7 ± 0.4 (10.0 ± 0.2)	48	2×10^5	0.06
Leu_{12}	5.0 ± 0.4	0.94 ± 0.09	0.74 ± 0.06	4.4 ± 0.1 (ND)	36	9×10^5	0.02
Leu_9	3.2 ± 0.3	0.77 ± 0.04	0.55 ± 0.02	3.7 ± 0.2 (10.0 ± 0.2)	29	4×10^5	0.04
Asn_1Leu_9	4.4 ± 0.6	0.86 ± 0.06	1.17 ± 0.07	1.2 ± 0.1 (9.2 ± 0.2)	15	4×10^6	0.003
average	4.5 ± 0.5	0.82 ± 0.06					

[a] Molar ratio of peptide to SERCA. The average value was calculated for all reconstitutions and corresponds to approximately 4.5 mol of peptide/mol of SERCA. [b] Weight ratio of lipid to protein. The average value was calculated for all reconstitutions and corresponds to approximately 120 mol of lipid/mol of SERCA. [c] The pCa values reported in the text have been converted to micromolar Ca^{2+} concentrations. [d] Maximal activity (micromoles per milligram per minute). In parentheses is the maximal activity measured in the presence of 1 mg/mL detergent ($C_{12}E_8$). [e] For the kinetic analysis, the reaction scheme and initial rate constants were taken from Cantilina et al. (*6*). The constants listed above correspond to the final fit (see Experimental Procedures and Results) for the forward and reverse rates for a conformational transition in SERCA upon binding the first Ca^{2+} ion.

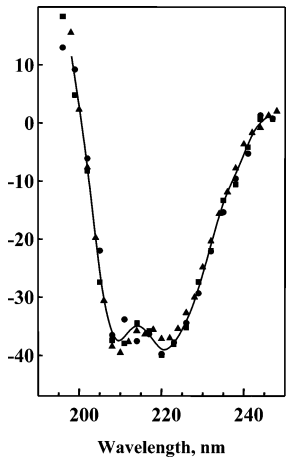

FIGURE 3: Comparative circular dichroism studies of the Leu_4, Leu_7, and Leu_9 peptides. CD spectra were recorded for the Leu_4 (●), Leu_7 (■), and Leu_9 (▲) peptides reconstituted into SOPC lipid vesicles. Molar ellipticities (degrees square centimeters per decimole $\times 10^{-3}$) are plotted versus wavelength (nanometers). The data for the three peptides were indistinguishable, and a simple spline curve of the combined data is shown (—). The curve is not an estimate of helical content.

We then tested the ability of Leu_{18} and Leu_{24} to alter the K_{Ca} of SERCA in co-reconstituted proteoliposomes (Figure 4 and Table 1). The Leu_{18} peptide, which included the lysine capping residues, had no effect on the calcium affinity of SERCA. Therefore, this peptide served as a negative control for all further studies. In contrast, the Leu_{24} peptide significantly altered the calcium affinity of SERCA. The observed K_{Ca} of SERCA was 0.38 μM Ca^{2+} in the presence of Leu_{18} and 0.54 μM Ca^{2+} in the presence of Leu_{24}. The effect of Leu_{24} on the observed K_{Ca} had a high statistical probability of being distinct from SERCA in the absence of peptide ($p < 10^{-2}$). On the basis of the behavior of Leu_{18} and Leu_{24} in our co-reconstitution system, we conclude that a uniform hydrophobic peptide can alter the apparent calcium affinity of SERCA with a length requirement that is similar to that of wild-type PLB.

Leucine-Containing Polyalanine Peptides. Synthetic leucine-alanine peptides have also been utilized as models for transmembrane α-helices (*16*, *17*). In our studies, three peptides were synthesized: acetyl-K_2-$(LAAAAAA)_3$LAA-K_2-amide, acetyl-K_2-$(LAAALAA)_3$LAA-K_2-amide, and acetyl-K_2-$(LA)_{12}$-K_2-amide (designated Leu_4, Leu_7, and Leu_{12}, respectively). These peptides adopt predominantly helical conformations (Figure 3), but they possess more limited hydrophobic surfaces than a polyleucine helix. The leucine residues in the Leu_4 and Leu_7 peptides line one face of a transmembrane α-helix, while Leu_{12} has a broader distribution of leucine residues (Figure 1). For instance, the Leu_7 peptide has leucine residues at positions equivalent to Leu^{28}, Phe^{32}, Phe^{35}, Leu^{39}, Leu^{42}, Cys^{46}, and Val^{49} in a sequence comparison with wild-type PLB.

We tested the ability of Leu_4, Leu_7, and Leu_{12} to alter the K_{Ca} of SERCA in co-reconstituted proteoliposomes (Figure 4 and Table 1). All three peptides significantly altered the calcium affinity of SERCA. The observed K_{Ca} of SERCA was 0.49 μM Ca^{2+} in the presence of Leu_4, 0.50 μM Ca^{2+} in the presence of Leu_7, and 0.74 μM Ca^{2+} in the presence of Leu_{12}. The effects of the peptides on the observed K_{Ca} had a high statistical probability of being distinct from SERCA in the absence of peptide ($p < 10^{-2}$). On the basis of the behavior of Leu_4, Leu_7, and Leu_{12} in our co-reconstitution system, we conclude that helical transmembrane peptides with limited hydrophobic surfaces can alter the apparent calcium affinity of SERCA. While the Leu_4 and Leu_7 peptides only moderately affected the calcium affinity, the Leu_{12} peptide was a more potent inhibitor comparable to wild-type PLB (*9*).

Leucine-Alanine Peptide Designed To Mimic PLB. We next synthesized a peptide that contained all of the naturally occurring leucine residues in the transmembrane domain of PLB, with all other residues substituted with alanine (Figure 1; acetyl-K_2-LAALAAAAALALAALLLAAAAAALL-K_2-amide, designated Leu_9). The configuration of leucine residues in PLB does not conform to a uniform hydrophobic surface, and three of these leucine residues are considered essential (Leu^{31}, Leu^{42}, and Leu^{52}). We tested the ability of Leu_9 to alter the K_{Ca} of SERCA in co-reconstituted proteoliposomes (Figure 5 and Table 1). The Leu_9 peptide significantly altered the calcium affinity of SERCA, yielding a K_{Ca} of 0.55 μM Ca^{2+}. The effect of Leu_9 on the observed

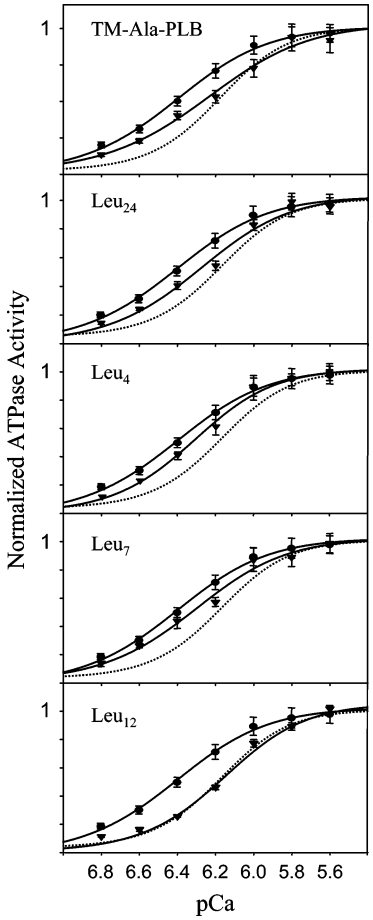

FIGURE 4: ATPase activity as a function of free calcium concentration. SERCA was co-reconstituted in the absence (●) and presence (▼) of synthetic peptide inhibitors (TM-Ala-PLB, Leu_{24}, Leu_4, Leu_7, and Leu_{12}). The data are plotted as normalized ATPase specific activity vs pCa, and each data point is the mean ± the standard error of the mean [$n = 17$ (●); $n = 3-5$ (▼)]. The K_{Ca} and V_{max} values were calculated by fitting the data to the Hill equation (fits not shown) and are reported in Table 1. The K_{Ca} values in pCa units were 6.42 ± 0.01 (control), 6.23 ± 0.02 (TM-Ala-PLB) 6.27 ± 0.02 (Leu_{24}), 6.31 ± 0.01 (Leu_4), 6.30 ± 0.01 (Leu_7), and 6.13 ± 0.04 (Leu_{12}). Comparable data are shown for wild-type PLB (- - -), where the K_{Ca} was 6.17 ± 0.02 pCa units (*9*). The curves were obtained using Dynafit to fit the data to the model of Cantilina et al. (*6*) as described in Experimental Procedures and Table 1.

K_{Ca} had a high statistical probability of being distinct from SERCA in the absence of peptide ($p < 10^{-2}$). The inhibitory capacity of the Leu_9 peptide was comparable to that of Leu_{24}, stronger than that of either Leu_4 or Leu_7, and weaker than that of Leu_{12}. We conclude that quite simple hydrophobic peptides are capable of altering the calcium affinity of SERCA. However, the potency and topology of Leu_9 and Leu_{12} suggest that the interaction interface between the peptide and SERCA is complex and involves residues distributed over much of the surface of the transmembrane helical peptide (*43*).

We sought to determine if these peptides mimicked the inhibition by the transmembrane domain of PLB. To test this hypothesis, we synthesized a peptide that contained all of the naturally occurring leucine residues in the transmembrane domain of PLB, as well as the essential residue Asn^{34} (Figure 1; acetyl-K_2-LAALAANAALALAALLLAAAAAA-LL-K_2-amide, designated Asn_1Leu_9). The nine leucine residues and Asn^{34} occupy their native positions, based on a

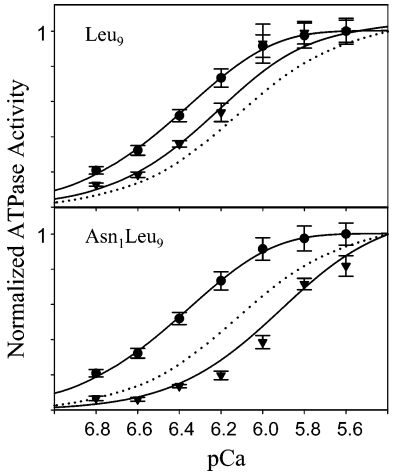

FIGURE 5: ATPase activity as a function of free calcium concentration. SERCA was co-reconstituted in the absence (●) and presence (▼) of synthetic peptide inhibitors (Leu_9 and Asn_1Leu_9). The data are plotted as normalized ATPase specific activity vs pCa, and each data point is the mean ± the standard error of the mean [$n = 17$ (●); $n = 3-5$ (▲)]. The K_{Ca} and V_{max} values were calculated by fitting the data to the Hill equation (fits not shown) and are reported in Table 1. The K_{Ca} values in pCa units were 6.42 ± 0.01 (control), 6.26 ± 0.02 (Leu_9), and 5.93 ± 0.03 (Asn_1Leu_9). Comparable data are shown for wild-type PLB (- - -), where the K_{Ca} is 6.17 ± 0.02 pCa units (*9*). Curves were obtained from fitting the data to the kinetic model of Cantilina et al. (*6*) as described.

sequence alignment with wild-type PLB. We tested the ability of Asn_1Leu_9 to alter the K_{Ca} of SERCA in co-reconstituted proteoliposomes (Figure 5 and Table 1). The Asn_1Leu_9 peptide proved to be a very potent inhibitor of SERCA, yielding a K_{Ca} of 1.17 μM Ca^{2+} (a 3-fold decrease in calcium affinity). The peptide also reversibly altered the maximal activity of SERCA, decreasing V_{max} to approximately 70% compared to control. The effect of the Asn_1Leu_9 peptide on the observed K_{Ca} and V_{max} had a high statistical probability of being distinct from SERCA in the absence of peptide ($p < 10^{-2}$). This Asn_1Leu_9 peptide was the most potent inhibitor observed in our co-reconstituted proteoliposomes, surpassing the PLB gain-of-function mutants (*7*, *9*). The large change in the inhibitory potency of Asn_1Leu_9 compared to that of Leu_9 suggests that these peptides occupy the same binding site and utilize an inhibitory mechanism analogous to that of wild-type PLB.

Given that the Asn_1Leu_9 peptide was designed from the PLB sequence, this peptide also bears homology to SLN (*44*). Furthermore, the side chain distribution of the Asn_1Leu_9 peptide suggested that it might be small enough to form a ternary complex with wild-type PLB and SERCA, as has been reported for SLN (*5*). To test this hypothesis, we compared the level of inhibition observed for (i) a 1:1 molar stoichiometry of wild-type PLB to SERCA, (ii) a 1:1 molar stoichiometry of Asn_1Leu_9 to SERCA, and (iii) a 1:1:1 molar stoichiometry of wild-type PLB to Asn_1Leu_9 to SERCA. The result of this experiment (Table 2) showed that the combined effect of wild-type PLB and Asn_1Leu_9 was a synergistic shift in the apparent calcium affinity of SERCA. The presence of equimolar amounts of both wild-type PLB and Asn_1Leu_9 shifted the calcium affinity of SERCA to 1.62 μM Ca^{2+}. Therefore, the Asn_1Leu_9 peptide appeared to mimic SLN and was capable of forming a ternary, superinhibitory complex with wild-type PLB and SERCA. In terms of the observed

Table 2: SERCA Superinhibition by Asn_1Leu_9 and Wild-Type PLB

	K_{Ca}				kinetic analysis[b]		
peptide[a]	pCa	ΔpCa	$[Ca^{2+}]$ (μM)	V_{max}	$B_{forward}$	$B_{reverse}$	sum of squares
control	6.42 ± 0.01		0.38	4.3 ± 0.3	30	40	0.002
wild-type PLB	6.28 ± 0.01	−0.13	0.52	3.9 ± 0.1	27	4×10^5	0.03
Asn_1Leu_9	6.05 ± 0.03	−0.37	0.89	3.5 ± 0.1	25	2×10^6	0.02
wild-type PLB and Asn_1Leu_9	5.80 ± 0.01	−0.61	1.62	4.0 ± 0.1	31	5×10^6	0.004

[a] SERCA was co-reconstituted in the absence of peptide (control), in the presence of 1 molar equiv of wild-type PLB (wild-type PLB), in the presence of 1 molar equiv of peptide (Asn_1Leu_9), and in a 1:1:1 SERCA:PLB:peptide molar ratio (wild-type PLB and Asn_1Leu_9). [b] The kinetic analysis is the same as that described in Table 1 (see Experimental Procedures and Results).

effect on K_{Ca}, the ternary complex had a high statistical probability ($p < 10^{-2}$) of being distinct from SERCA alone, from SERCA with wild-type PLB, and from SERCA with Asn_1Leu_9 peptide.

Effects on the Maximal Activity and Cooperativity of SERCA. An important remaining question in our peptide studies was the variable effect on the V_{max} of SERCA, which was dependent on the peptide under consideration (Table 1). Independent effects of the peptides were observed on the V_{max} and K_{Ca} of SERCA. Leu_{18} decreased V_{max} and had no effect on K_{Ca}, while Leu_{12} had no effect on V_{max} and significantly altered K_{Ca}. In summary, three peptides had no effect on V_{max} (TM-Ala-PLB, Leu_{12}, and Leu_9), two peptides activated V_{max} (Leu_4 and Leu_7), and three peptides suppressed V_{max} (Leu_{18}, Leu_{24}, and Asn_1Leu_9). To rule out nonspecific effects on SERCA, we tested whether solubilizing amounts of detergent could reverse the observed activation or suppression of V_{max} by the peptides. Solubilizing amounts of the nonionic detergent, $C_{12}E_8$, have been shown to reverse the inhibition of SERCA by PLB and cause a 2−3-fold stimulation of SERCA activity (*10*, *45*, *46*). As previously observed by others, the V_{max} effects were completely reversible in the presence of detergent (Table 1). Therefore, we conclude that the activation or suppression of SERCA activity at saturating calcium concentrations is a specific effect of the peptides. However, a more exhaustive study of peptide sequence variation on SERCA maximal activity would be required to fully understand this effect.

The Hill coefficients, n_H, were also calculated from the ATPase curves. For reconstituted SERCA, n_H was 1.8 ± 0.2, in agreement with published values ranging from 1.5 to 2 (*8*, *47*−*49*). The n_H for SERCA reconstituted with PLB was slightly higher, 2.1 ± 0.2. This cooperativity is maintained when SERCA is reconstituted with the peptides. The n_H values ranged from a minimum of 1.6 for SERCA in the presence of the Leu_{18} peptide to a maximum of 2.1 for SERCA in the presence of the Leu_9 peptide. The n_H values for wild-type PLB and all peptides were not statistically different from those of the control samples (SERCA alone).

Molar Stoichiometry of Peptides. If the peptides studied herein actually mimic PLB, one would expect them to inhibit SERCA at an approximate 1:1 molar stoichiometry of peptide to SERCA (*50*, *51*). We tested this hypothesis for a representative subset of peptides, including Leu_4, Leu_9, and Asn_1Leu_9. We measured the observed calcium affinity over a range of peptide:SERCA molar ratios from 0.5:1 to 5:1 (Figure 6). For all three peptides that were tested, the effect on the calcium affinity of SERCA was maximal at 1 mol of peptide/mol of SERCA, similar to previous observations with wild-type PLB (*50*, *51*). Therefore, we conclude that the

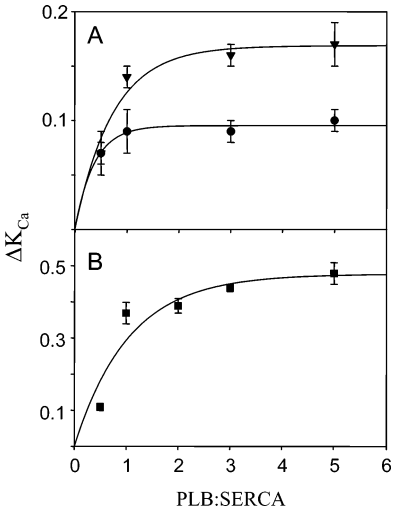

FIGURE 6: Molar stoichiometry of the Leu_4, Leu_9, and Asn_1Leu_9 peptides and inhibition of SERCA. Relationship between the shift in the apparent calcium affinity (ΔK_{Ca}) of SERCA and the molar stoichiometry of peptides in the co-reconstituted proteoliposomes. (A) Data are shown for the Leu_4 (●) and Leu_9 (▼) peptides. (B) Data are shown for the Asn_1Leu_9 (■) peptide. Each peptide data point is the mean ± the standard error of the mean ($n = 3$−5).

synthetic peptides possess characteristics reminiscent of SERCA inhibition by PLB: the helix length and hydrophobicity, the role of an essential amino acid, and the molar stoichiometry of inhibition all mimic PLB function.

Kinetic Analysis. In the reaction scheme for calcium transport by SERCA, a slow transition (E·Ca → E′·Ca) that increases the cooperativity for calcium binding and activates the enzyme has been postulated (*6*). The rate constants for this reaction step ($B_{forward}$ and $B_{reverse}$) increase in the presence of PLB, resulting in the shift in calcium affinity observed experimentally. We used this reaction scheme (*6*) and Dynafit (*35*) to simulate our activity curves (ATP hydrolysis vs calcium concentration) in the absence and presence of peptides. Dynafit was used to systematically vary each forward and reverse rate constant in the reaction scheme in an effort to simulate our activity curves. The experimentally observed changes in maximal activity and calcium affinity in the presence of peptides could be completely explained by altering the magnitude of the forward and reverse rate constants for step B (isomeric transition following calcium binding). The results of this analysis are summarized in Table 1. For wild-type PLB, as well as the peptides, the shift in calcium affinity was attributed to a large increase in the reverse rate constant, strongly favoring E·Ca over E′·Ca. In addition, the changes in maximal activity correlated with changes in the forward rate constant; peptides that decreased V_{max} also decreased the forward rate constant and favored

E·Ca, and peptides that increased V_{max} also increased the forward rate constant and favored E′·Ca. On the basis of this analysis, the peptides appeared to mimic the mechanistic behavior of wild-type PLB.

DISCUSSION

The transmembrane domain of PLB, in the absence of the cytoplasmic domain, has been shown to retain approximately 70% of the inhibitory function of wild-type PLB (*38*, *41*). The amino acid sequence of this domain is practically invariant across mammalian species, suggesting a precise requirement for the physical interaction between PLB and SERCA, as well as between PLB monomers. In the transmembrane domain of PLB, leucine is the most common amino acid (9 of 28 residues are leucines). Of these leucine residues, three are considered essential (Leu^{31}, Leu^{42}, and Leu^{52}) in that they yield loss-of-function mutants with less than half the inhibitory function of wild-type PLB when mutated to alanine (*7*). Three additional leucine residues (Leu^{37}, Leu^{44}, and Leu^{51}) have been implicated in PLB pentamer formation (*13*). The role of individual amino acids appears to be context-dependent, further complicating things; i.e., the few existing studies using PLB double mutants indicate that some loss-of-function mutations can at least be partially reversed by second site mutations (*7*, *11*, *12*). Given the prevalence of hydrophobic residues in the primary sequence of PLB, we varied the complexity of the hydrophobic surface and assessed the inhibitory interaction with SERCA. The peptides Leu_4, Leu_7, Leu_9, and Leu_{24} were relatively weak but significant inhibitors of SERCA, with approximately 50−60% of the inhibitory capacity of wild-type PLB. The Leu_{12} peptide was a stronger inhibitor, comparable to wild-type PLB. Surprisingly, adding back essential amino acid Asn^{34} to the Leu_9 peptide resulted in one of the most potent SERCA inhibitors we have observed. The Asn_1Leu_9 peptide was a more potent inhibitor than any of the known PLB gain-of-function mutants (*7*, *9*), and this inhibitory potency increased further in a ternary interaction with wild-type PLB and SERCA.

The experimental evidence suggests that the model peptides utilized in this study mimic the transmembrane domain of PLB. First, the majority of peptides form oligomers as diagnosed by SDS−PAGE, the major diagnostic tool used to characterize PLB oligomerization (*7*, *52*). For most peptides, the major species present were dimers and monomers, although higher-order oligomers were also observed. This is somewhat surprising, given that the leucine-isoleucine residues implicated in PLB pentamer formation were not fully occupied in this set of peptides. Nonetheless, recent structural evidence suggests that at least one monomeric mutant of PLB (Ile^{40} to Ala) is capable of forming pentamers (*53*). Thus, SDS−PAGE alone may be insufficient for diagnosing the stability of peptide oligomers. Second, the peptides shifted the apparent calcium affinity of SERCA in a fashion similar to that of wild-type PLB. While the majority of peptides were weak inhibitors, they were statistically significant. The shift in calcium affinity was due to a change in the rate constants for a characteristic step in the SERCA reaction scheme for calcium binding, another hallmark of PLB function. The original work by Inesi and colleagues (*6*) found that PLB decreased both the forward and reverse rate constants for the E·Ca → E′·Ca isomeric transition with no change in the equilibrium constant. In contrast, our simulations required that we greatly increase the reverse rate constant while only slightly altering the forward rate constant, yielding equilibrium constants of 0.75 for SERCA alone and 6×10^{-5} for SERCA in the presence of PLB. This result is consistent with a recent study in which a decrease in this equilibrium constant was necessary to simulate the shift in the calcium dependence of SERCA activity in the presence of PLB (*54*). Third, the potent inhibition of the Asn_1Leu_9 peptide was consistent with the essential role of Asn^{34} in PLB function. While we expected a significant increase in the level of inhibition compared to that of the Leu_9 peptide, the potent inhibition by this peptide was not predicted on the basis of our current understanding of PLB structure and function.

Taken together, the inhibitory properties of these synthetic peptides allowed us to draw conclusions about the essential sequence elements required for SERCA inhibition. First, a uniform hydrophobic surface on a canonical transmembrane α-helix that completely traverses the membrane bilayer meets a partial requirement for SERCA inhibition. A polyleucine helix 24 amino acids in length was shown to partially mimic the inhibitory properties of PLB. A shorter polyleucine helix of 18 amino acids did not alter the apparent calcium affinity of SERCA, despite meeting a minimal requirement for traversing a lipid bilayer (*55*). The Leu_{18} peptide bears a striking resemblance to SLN, which possesses a 19-amino acid transmembrane domain flanked by polar residues (Figure 1B). Interestingly, both Leu_{18} and SLN decrease the V_{max} of SERCA, and perhaps this is due to the polar residues flanking their transmembrane domains. In contrast, only SLN alters the calcium affinity of SERCA (*5*, *44*). It is also possible that the rigidity of a polyleucine helix and the fact that shorter helices are not tilted in the membrane are responsible for the lack of an effect of Leu_{18} on the calcium affinity of SERCA. Second, the uniform hydrophobic surface required for SERCA inhibition can be quite limited. The Leu_4 and Leu_7 peptides possessed only four and seven leucine residues lining one face of a transmembrane α-helix, respectively. Nonetheless, these two peptides were weak but significant inhibitors of SERCA with almost 50% of wild-type PLB function. The Leu_4 sequence preserves Leu^{28} and Leu^{42} and contains leucine residues at the equivalent positions of Phe^{35} and Val^{49} in wild-type PLB. The Leu_7 sequence preserves Leu^{28}, Leu^{39}, and Leu^{42} and contains leucine residues at the equivalent positions of Phe^{32}, Phe^{35}, Cys^{46}, and Val^{49} in wild-type PLB. Phe^{35}, Leu^{42}, and Val^{49} are essential residues in wild-type PLB (*7*). The lack of inhibition by Leu_{18} suggests that the lysine caps do not effect the calcium affinity of SERCA; however, we cannot rule out effects of these lysine residues for the longer peptides.

Consistent with previous observations, the hydrophobic surface required for SERCA inhibition involves amino acid residues distributed around the circumference of the transmembrane peptide (*43*). The Leu_9 and Leu_{12} peptides had complex topologies of leucine residues distributed over the surface of the transmembrane α-helix. The Leu_{12} peptide had a level of inhibition similar to that of wild-type PLB, while the Leu_9 peptide retained 60% of wild-type PLB function. The Leu_9 sequence preserves all of the naturally occurring leucine residues in the transmembrane domain of wild-type PLB (Leu^{28}, Leu^{31}, Leu^{37}, Leu^{39}, Leu^{42}, Leu^{43}, Leu^{44}, Leu^{51},

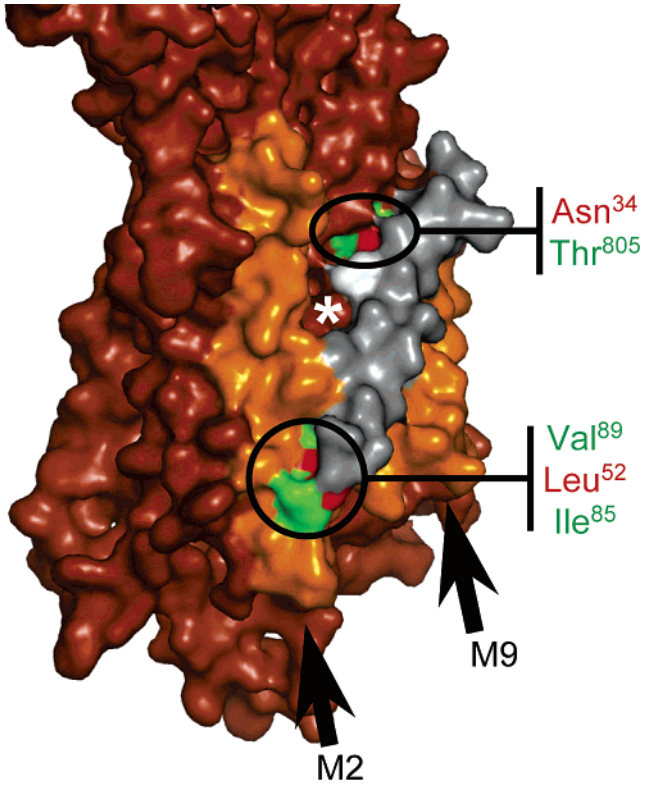

FIGURE 7: Potential interactions between the E2 form of SERCA and the Asn_1Leu_9 peptide. Surface representation of SERCA (brown; M2 and M9 are colored orange) and Asn_1Leu_9 (gray) as viewed with M2 of SERCA in the foreground. The interaction between Asn^{34} and Thr^{805} appears to be more efficient due to the reduced steric hindrance provided by the alanine side chains (asterisk; Leu^{37} is colored white). The side chains of Leu^{31}, Leu^{42}, and Leu^{52} are buried in hydrophobic pockets formed by the transmembrane domain of SERCA. The interaction of Leu^{52} in the Asn_1Leu_9 peptide with Ile^{85} and Val^{89} of SERCA is shown above.

and Leu^{52}). The Leu_{12} sequence preserves Leu^{28}, Leu^{42}, and Leu^{44} and contains leucine residues at the equivalent positions of Asn^{30}, Phe^{32}, Asn^{34}, Cys^{36}, Ile^{38}, Ile^{40}, Cys^{46}, Ile^{48}, and Met^{50} in wild-type PLB. At present, the stronger inhibition observed for Leu_{12} compared to Leu_{24} is unexplained. However, the potent inhibitory capacity of Leu_{12} may be due to the fact that more of the essential amino acid positions of PLB are occupied by leucines (Asn^{34}, Ile^{38}, Leu^{42}, and Ile^{48}), while the alternating leucine-alanine sequence of Leu_{12} may provide greater side chain flexibility for recognizing and binding to a helical interface on SERCA. If this interpretation is correct, side chain flexibility combined with occupancy of essential positions may be the relevant features in the inhibitory interaction with SERCA.

Finally, we built a model for the interaction of Asn_1Leu_9 with SERCA (Figure 7) in an effort to decipher the sequence elements that contribute to the potent inhibition by this peptide. The model was based on the interaction of the transmembrane domain of PLB [1ZLL (*13*)], as dictated by the available cross-linking data (*56*−*59*). In our model, peptide residues Leu^{37} and Leu^{44} face SERCA but make only weak hydrophobic interactions, while peptide residues Leu^{28}, Leu^{39}, Leu^{43}, and Leu^{51} face the lipid bilayer. The alanine side chains in the Asn_1Leu_9 peptide allow (i) Leu^{31} to pack against Trp^{932} of SERCA, (ii) unhindered interaction between Asn^{34} and Thr^{805} of SERCA, (iii) Leu^{42} to insert efficiently into a pocket formed by Leu^{943}, Leu^{946}, and Leu^{953} of SERCA, and (iv) Leu^{52} to insert efficiently into a pocket formed by Ile^{85} and Val^{89} of SERCA. The end result is increased surface complementarity and decreased steric hindrance that favors the interaction of the essential Leu^{31}, Asn^{34}, Leu^{42}, and Leu^{52} residues. Hydrogen bonding between Asn^{34} and Thr^{805} is suggested to orient the transmembrane helix of PLB in the inhibitory interaction with SERCA (*58*). If this is correct, the Asn_1Leu_9 peptide may be more effective at making this hydrogen bond, while the van der Waals contacts of Leu^{31}, Leu^{42}, and Leu^{52} stabilize the SERCA-bound state along the length of the helix. In the model, there are hydrophobic pockets that would readily accommodate essential residues Phe^{35}, Ile^{38}, Ile^{48}, and Val^{49} (not present in this peptide), further stabilizing the complex. This finding suggests the following sequence elements for SERCA inhibition: an essential asparagine residue and a series of hydrophobic residues at key positions along the transmembrane helix that position Asn^{34} for hydrogen bonding to Thr^{805}.

ACKNOWLEDGMENT

We thank Dr. Robert Parker for peptide synthesis, Drs. Ruthven N. A. H. Lewis and Ronald N. McElhaney for helpful discussions, and Dr. Ariel Caride for help with Dynafit kinetic analyses.

REFERENCES

1. Kirchberger, M. A., Tada, M., and Katz, A. M. (1975) Phospholamban: A regulatory protein of the cardiac sarcoplasmic reticulum, *Recent Adv. Stud. Card. Struct. Metab. 5*, 103−15.
2. Katz, A. M., Repke, D. I., Kirchberger, M. A., and Tada, M. (1974) Calcium-binding sites and calcium uptake in cardiac microsomes: Effects of varying Ca^{2+} concentration, and of an adenosine-3′,5′-monophosphate-dependent protein kinase, *Recent Adv. Stud. Cardiac Struct. Metab. 4*, 427−36.
3. Wawrzynow, A., Theibert, J. L., Murphy, C., Jona, I., Martonosi, A., and Collins, J. H. (1992) Sarcolipin, the "proteolipid" of skeletal muscle sarcoplasmic reticulum, is a unique, amphipathic, 31-residue peptide, *Arch. Biochem. Biophys. 298*, 620−3.
4. Minamisawa, S., Wang, Y., Chen, J., Ishikawa, Y., Chien, K. R., and Matsuoka, R. (2003) Atrial chamber-specific expression of sarcolipin is regulated during development and hypertrophic remodeling, *J. Biol. Chem. 278*, 9570−5.
5. Asahi, M., Sugita, Y., Kurzydlowski, K., Leon, S. D., Tada, M., Toyoshima, C., and MacLennan, D. (2003) Sarcolipin regulates sarco(endo)plasmic reticulum Ca^{2+}-ATPase (SERCA) by binding to transmembrane helices alone or in association with phospholaman, *Proc. Natl. Acad. Sci. U.S.A. 100*, 5040−5.
6. Cantilina, T., Sagara, Y., Inesi, G., and Jones, L. R. (1993) Comparative studies of cardiac and skeletal sarcoplasmic reticulum ATPases: Effect of phospholamban antibody on enzyme activation, *J. Biol. Chem. 268*, 17018−25.
7. Kimura, Y., Kurzydlowski, K., Tada, M., and MacLennan, D. H. (1997) Phospholamban inhibitory function is enhanced by depolymerization, *J. Biol. Chem. 272*, 15061−4.
8. Toyofuku, T., Kurzydlowski, K., Tada, M., and MacLennan, D. H. (1994) Amino acids Glu^2 to Ile^{18} in the cytoplasmic domain of phospholamban are essential for functional association with the Ca^{2+}-ATPase of sarcoplasmic reticulum, *J. Biol. Chem. 269*, 3088−94.
9. Trieber, C. A., Douglas, J., Afara, M., and Young, H. S. (2005) The effects of mutation on the regulatory properties of phospholamban in co-reconstituted membranes, *Biochemistry 44*, 3289−97.
10. Reddy, L., Cornea, R., Winters, D., McKenna, E., and Thomas, D. (2003) Defining the molecular components of calcium transport regulation in a reconstituted membrane system, *Biochemistry 42*, 4585−92.
11. Asahi, M., Kimura, Y., Kurzydlowski, K., Tada, M., and MacLennan, D. H. (1999) Transmembrane helix M6 in sarco(endo)-

plasmic reticulum Ca^{2+}-ATPase forms a functional interaction site with phospholamban. Evidence for physical interactions at other sites, *J. Biol. Chem. 274*, 32855−62.
12. Kimura, Y., Asahi, M., Kurzydlowski, K., Tada, M., and MacLennan, D. H. (1998) Phospholamban domain Ib mutations influence functional interactions with the Ca^{2+}-ATPase isoform of cardiac sarcoplasmic reticulum, *J. Biol. Chem. 273*, 14238−41.
13. Oxenoid, K., and Chou, J. (2005) The structure of phospholamban pentamer reveals a channel-like architecture in membranes, *Proc. Natl. Acad. Sci. U.S.A. 102*, 10870−5.
14. Zhang, Y.-P., Lewis, R. N. A. H., Hodges, R. S., and McElhaney, R. N. (1992) FTIR spectroscopic studies of the conformation and amide hydrogen exchange of a peptide model of the hydrophobic transmembrane α-helices of membrane proteins, *Biochemistry 31*, 11572−8.
15. Zhang, Y.-P., Lewis, R. N. A. H., Hodges, R. S., and McElhaney, R. N. (1992) Interaction of a peptide model of a hydrophobic transmembrane α-helical segment of a membrane protein with phosphatidylcholine bilayers: Differential scanning calorimetric and FTIR spectroscopic studies, *Biochemistry 31*, 11579−88.
16. Zhang, Y.-P., Lewis, R. N. A. H., Henry, G. D., Sykes, B. D., Hodges, R. S., and McElhaney, R. N. (1995) Peptide models of helical hydrophobic transmembrane segments of membrane proteins. 1. Studies of the conformation, intrabilayer orientation, and amide hydrogen exchangeability of Ac-K_2-$(LA)_{12}$-K_2-amide, *Biochemistry 34*, 2348−61.
17. Zhang, Y.-P., Lewis, R. N. A. H., Hodges, R. S., and McElhaney, R. N. (1995) Peptide models of helical hydrophobic transmembrane segments of membrane proteins. 2. Differential scanning calorimetric and FTIR spectroscopic studies of the interaction of Ac-K_2-$(LA)_{12}$-K_2-amide with phosphatidylcholine bilayers, *Biochemistry 34*, 2362−71.
18. Lewis, R. N. A. H., Zhang, Y.-P., Liu, F., and McElhaney, R. N. (2002) Mechanisms of the interaction of α-helical transmembrane peptides with phospholipid bilayers, *Bioelectrochemistry 56*, 135−40.
19. Liu, F., Lewis, R., Hodges, R., and McElhaney, R. (2002) Effect of variations in the structure of a polyleucine-based α-helical transmembrane peptide on its interaction with phosphatidylcholine bilayers, *Biochemistry 41*, 9197−207.
20. Liu, F., Lewis, R. N. A. H., Hodges, R. S., and McElhaney, R. N. (2004) Effect of variations in the structure of a polyleucine-based α-helical transmembrane peptide on its interaction with phosphatidylethanolamine bilayers, *Biophys. J. 87*, 2470−82.
21. Liu, F., Lewis, R. N. A. H., Hodges, R. S., and McElhaney, R. N. (2004) Effect of variations in the structure of a polyleucine-based α-helical transmembrane peptide on its interaction with phosphatidylglycerol bilayers, *Biochemistry 43*, 3679−87.
22. Davis, J., Clare, D., Hodges, R., and Bloom, M. (1983) Interaction of a synthetic amphiphilic polypeptide and lipids in a bilayer structure, *Biochemistry 22*, 5298−305.
23. Hughes, G., Starling, A. P., Sharma, R. P., East, J. M., and Lee, A. G. (1996) An investigation of the mechanism of inhibition of the Ca^{2+}-ATPase by phospholamban, *Biochem. J. 318*, 973−9.
24. Warren, G. B., Toon, P. A., Birdsall, N. J. M., Lee, A. G., and Metcalfe, J. C. (1974) Reconstitution of a calcium pump using defined membrane components, *Proc. Natl. Acad. Sci. U.S.A. 71*, 622−6.
25. Eletr, S., and Inesi, G. (1972) Phospholipid orientation in sarcoplasmic reticulum membranes: Spin-label ESR and proton NMR studies, *Biochim. Biophys. Acta 282*, 174−9.
26. Stokes, D. L., and Green, N. M. (1990) Three-dimensional crystals of Ca-ATPase from sarcoplasmic reticulum: Symmetry and molecular packing, *Biophys. J. 57*, 1−14.
27. Reddy, L. G., Jones, L. R., Cala, S. E., O'Brian, J. J., Tatulian, S. A., and Stokes, D. L. (1995) Functional Reconstitution of Recombinant Phospholamban with Rabbit Skeletal Ca-ATPase, *J. Biol. Chem. 270*, 9390−7.
28. Young, H. S., Rigaud, J. L., Lacapere, J. J., Reddy, L. G., and Stokes, D. L. (1997) How to make tubular crystals by reconstitution of detergent-solubilized Ca^{2+}-ATPase, *Biophys. J. 72*, 2545−58.
29. Young, H. S., Reddy, L. G., Jones, L. R., and Stokes, D. L. (1998) Co-reconstitution and co-crystallization of phospholamban and Ca^{2+}-ATPase, *Ann. N.Y. Acad. Sci. 853*, 103−15.
30. Young, H. S., Jones, L. R., and Stokes, D. L. (2001) Locating phospholamban in co-crystals with Ca^{2+}-ATPase by cryoelectron microscopy, *Biophys. J. 81*, 884−94.
31. Smith, B. J. (2002) in *The Protein Protocols Handbook* (Walker, J. M., Ed.) pp 237−42, Humana Press, Totowa, NJ.
32. Chester, D. W., Herbette, L. G., Mason, R. P., Joslyn, A. F., and Triggle, D. J. (1987) Diffusion of dihydropyridine calcium channel antagonists in cardiac sarcolemmal lipid multibilayers, *Biophys. J. 52*, 1021−30.
33. Chen, P. S., Toribara, T. Y., and Warner, H. (1956) Microdetermination of phosphorous, *Anal. Chem. 28*, 1756−8.
34. Douglas, J. L., Trieber, C. A., Afara, M., and Young, H. S. (2005) Rapid, high-yield expression and purification of Ca^{2+}-ATPase regulatory proteins for high-resolution structural studies, *Protein Expression Purif. 40*, 118−25.
35. Kuzmic, P. (1996) Program DYNAFIT for the analysis of enzyme kinetic data: Application to HIV proteinase, *Anal. Biochem. 237*, 260−73.
36. Subczynski, W. K., Pasenkiewicz-Gierula, M., McElhaney, R. N., Hyde, J. S., and Kusumi, A. (2003) Molecular dynamics of 1-palmitoyl-2-oleoylphosphatidylcholine membranes containing transmembrane α-helical peptides with alternating leucine and alanine residues, *Biochemistry 42*, 3939−48.
37. dePlanque, M. R., and Killian, J. A. (2003) Protein−lipid interactions studied with designed transmembrane peptides: Role of hydrophobic matching and interfacial anchoring, *Mol. Membr. Biol. 20*, 271−84.
38. Karim, C. B., Marquardt, C. G., Stamm, J. D., Barany, B., and Thomas, D. D. (2000) Synthetic null-cysteine phospholamban analogue and the corresponding transmembrane domain inhibit the Ca-ATPase, *Biochemistry 39*, 10892−7.
39. Hellstern, S., Pegoraro, S., Karim, C., Lustig, A., Thomas, D., Moroder, L., and Engel, J. (2001) Sarcolipin, the shorter homologue of phospholamban, forms oligomeric structures in detergent micelles and in liposomes, *J. Biol. Chem. 276*, 30845−52.
40. Vorherr, T., Wrzosek, A., Chiesi, M., and Carafoli, E. (1993) Total synthesis and functional properties of the membrane intrinsic protein phospholamban, *Protein Sci. 2*, 339−47.
41. Kimura, Y., Kurzydlowski, K., Tada, M., and MacLennan, D. (1996) Phospholamban regulates the Ca^{2+}-ATPase through intramembrane interactions, *J. Biol. Chem. 271*, 21726−31.
42. Hutter, M., Krebs, J., Meiler, J., Griesinger, C., Carafoli, E., and Helms, V. (2002) A structural model of the complex formed by phospholamban and the calcium pump of sarcoplasmic reticulum obtained by molecular mechanics, *ChemBioChem 3*, 1200−8.
43. Cornea, R. L., Autry, J. M., Chen, Z., and Jones, L. R. (2000) Re-examination of the role of the leucine/isoleucine zipper residues of phospholamban in inhibition of the Ca^{2+}-pump of cardiac sarcoplasmic reticulum, *J. Biol. Chem. 275*, 41487−94.
44. Odermatt, A., Becker, S., Khanna, V. K., Kurzydlowski, K., Leisner, E., Pette, D., and MacLennan, D. H. (1998) Sarcolipin regulates the activity of SERCA1, the fast-twitch skeletal muscle sarcoplasmic reticulum Ca^{2+}-ATPase, *J. Biol. Chem. 273*, 12360−9.
45. Martins, O. B., and de-Meis, L. (1985) Stability and partial reactions of soluble and membrane-bound sarcoplasmic reticulum ATPase, *J. Biol. Chem. 260*, 6776−81.
46. Lu, Y., and Kirchberger, M. (1994) Effects of a nonionic detergent on calcium uptake by cardiac microsomes, *Biochemistry 33*, 5056−62.
47. Lytton, J., Westlin, M., Burk, S. E., Shull, G. E., and MacLennan, D. H. (1992) Functional comparisons between isoforms of the sarcoplasmic or endoplasmic reticulum family of calcium pumps, *J. Biol. Chem. 267*, 14483−9.
48. Antipenko, A. Y., Spielman, A. I., Sassaroli, M., and Kirchberger, M. A. (1997) Comparison of the kinetic effects of phospholamban phosphorylation and anti-phospholamban monoclonal antibody on the calcium pump in purified cardiac sarcoplasmic reticulum membranes, *Biochemistry 36*, 12903−10.
49. Toyofuku, T., Kurzydlowski, K., Lytton, J., and MacLennan, D. H. (1992) The nucleotide binding/hinge domain plays a crucial role in determining isoform-specific Ca^{2+} dependence of organellar Ca^{2+}-ATPases, *J. Biol. Chem. 267*, 14490−6.
50. Waggoner, J. R., Huffman, J., Griffith, B. N., Jones, L. R., and Mahaney, J. E. (2003) Improved expression and characterization of Ca^{2+}-ATPase and phospholamban in High-Five cells, *Protein Expression Purif. 34*, 56−67.
51. Ferrington, D., Yao, Q., Squier, T., and Bigelow, D. (2002) Comparable levels of Ca-ATPase inhibition by phospholamban in slow-twitch skeletal and cardiac sarcoplasmic reticulum, *Biochemistry 41*, 13289−96.

52. Lindemann, J. P., Jones, L. R., Hathaway, D. R., Henry, B. G., and Watanabe, A. M. (1983) β-Adrenergic stimulation of phospholamban phosphorylation and Ca^{2+}-ATPase activity in guinea pig ventricles, *J. Biol. Chem. 258*, 464−71.
53. Stokes, D. J., Pomfret, A. J., Rice, W. J., Glaves, J. P., and Young, H. S. (2006) Interactions between Ca^{2+}-ATPase and the pentameric form of phospholamban in two-dimensional co-crystals, *Biophys. J. 90*, 4213−23.
54. Li, J., Boschek, C. B., Xiong, Y., Sacksteder, C. A., Squier, T. C., and Bigelow, D. J. (2005) Essential role for Pro^{21} in phospholamban for optimal inhibition of the Ca-ATPase, *Biochemistry 44*, 16181−91.
55. Tiburu, E. K., Karp, E. S., Dave, P. C., Damodaran, K., and Lorigan, G. A. (2004) Investigating the dynamic properties of the transmembrane segment of phospholamban incorporated into phospholipid bilayers utilizing ^{2}H and ^{15}N solid-state NMR spectroscopy, *Biochemistry 43*, 13899−909.
56. Chen, Z., Stokes, D. L., Rice, W. J., and Jones, L. R. (2003) Spatial and dynamic interactions between phospholamban and the canine cardiac Ca^{2+} pump revealed with use of heterobifunctional cross-linking agents, *J. Biol. Chem. 278*, 48348−56.
57. Chen, Z., Stokes, D. L., and Jones, L. R. (2005) Role of leucine 31 of phospholamban in structural and functional interactions with the Ca^{2+} pump of cardiac sarcoplasmic reticulum, *J. Biol. Chem. 280*, 10530−9.
58. Toyoshima, C., Asahi, M., Sugita, Y., Khanna, R., Tsuda, T., and MacLennan, D. H. (2003) Modeling of the inhibitory interaction of phospholamban with the Ca^{2+} ATPase, *Proc. Natl. Acad. Sci. U.S.A. 100*, 467−72.
59. Chen, Z., Akin, B. L., Stokes, D. L., and Jones, L. R. (2006) Cross-linking of C-terminal residues of phospholamban to the Ca^{2+} pump of cardiac sarcoplasmic reticulum to probe spatial and functional interactions within the transmembrane domain, *J. Biol. Chem. 281*, 14163−72.

BI0523761